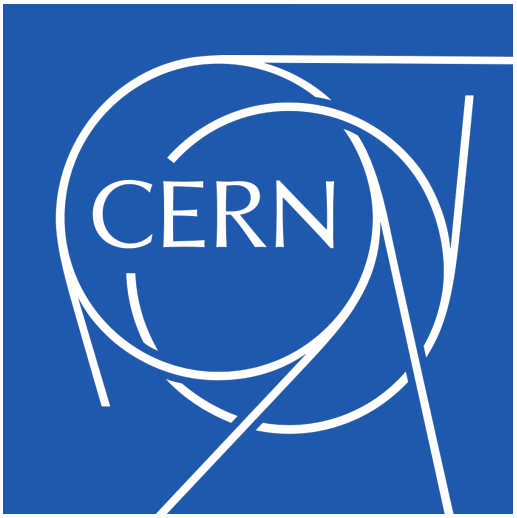

REPORT

Study of the $K^+ \to e^+ \nu e^+ e^-$ Decay with the NA62 Experiment

Anna Fehérkuti
Summer Student 2022
27 June - 23 September

Supervisors: Francesco Brizioli, Monica Pepe
EP-UFT, Small Medium Expt

Contents

Abstract

I joined a study concerning measurements of the branching ratio and the form factors of the rare decay $K^+ \to e^+ \nu e^+ e^-$ (Ke2ee) with the NA62 experiment.

With the data collected between 2016 and 2021, NA62 has currently a Ke2ee sample, large enough to significantly improve the state of the art. Preliminary studies show that it is possible to reach an almost background-free selection of Ke2ee decays, while maintaining a sizeable amount of signal events. In 2022, new data is being collected with the opportunity to achieve the largest Ke2ee sample in the world, suitable for improving the statistical uncertainty of the branching ratio and the form factors measurements.

I took part in the analysis of the 2017-2018 data sample: with the NA62 framework, producing histograms both with data and Monte Carlo simulations, building a signal selection, statistically interpreting the data and evaluating uncertainties.

1 Introduction

1.1 Brief Theoretical Background, Motivation

The motivation validating the importance of this work comes from kaon physics. The study of Ke2ee was performed in 2002 by the E865 experiment at BNL [2], with a statistics of 410 signal events including a background contamination of 10%. In this paper analysis of the same process on a larger datasample within the NA62 framework is shown.

A general $K^+ \to l^+ \nu l^+ l^-$ ($l = e, \mu$) decay is described by *Chiral Perturbation Theory* (ChPT), for which measurements provide both tests and inputs.

Within *Quantum Field Theory* (QFT) the probability of a process can be obtained by calculating the so-called *decay amplitude*. In this case it includes *inner bremsstrahlung*[1] (IB, see Figure 1) and *structure-dependent* components (SD, Figure 2) [1].

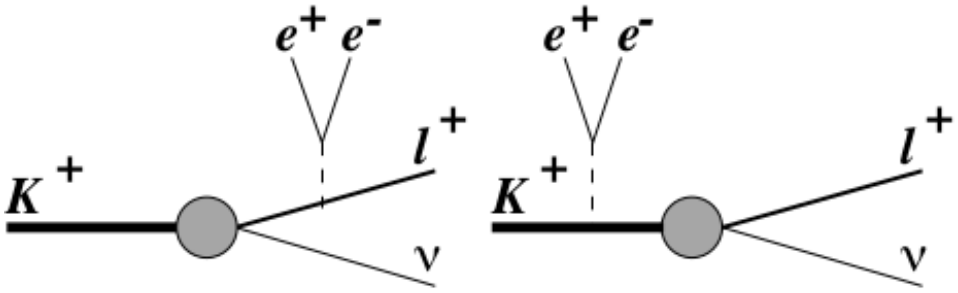

Figure 1: Different ways of inner bremsstrahlung (IB). [2]

The IB component is well-predicted by the $K^+ \to l^+\nu$ process (where l can be either electron or muon), while the SD one is parametrized by three *form factors* (F_V, F_A and R). A general kaon decay is sensitive for two of them due to being a weak decay; these are the vector (F_V) and the axial vector form factors (F_A). The third one (R) contributes only to decays with an e^- e^+ pair in the final state from virtual photon, which is the situation in this analysis. The studied process gets more interest if one consider the fact that due to *helicity suppression*[2] in this case the SD has a much stronger effect than IB.

1.2 The Branching Ratio

The *branching ratio* shows the probability of a decay channel as a ratio of the chosen channel with respect to all other possibilities. Since experimentally one cannot measure all the events, introduction of the so-called *normalization channel* is necessary. One takes the ratio between the two branching ratios making the denominators falling out, this is the *branching fraction* (Equation 1).

$$\frac{Br^{signal}}{Br^{norm}} = \frac{N^{signal}}{N^{norm}} \cdot \frac{\varepsilon^{norm}}{\varepsilon^{signal}} = \frac{N^{signal}}{N^{norm}} \cdot \frac{Acc^{norm}}{Acc^{signal}} \cdot \frac{Trig^{norm}}{Trig^{signal}}, \tag{1}$$

[1] Since the probability of this process is inversely proportional to the squared mass of the actual particle, it is more probable to have the left-hand side process in Figure 1, with positron in the final state.

[2] In a decay with $l^+\nu$ in the final state, for massless particles both have to own negative helicity, but in weak theory the antiparticle l^+ has to own positive chirality, which is the same as helicity for massless particles. This way as much the mass of a particle deviates from zero, this process is less and less suppressed. Therefore one has more suppression for positrons than for muons in this case.

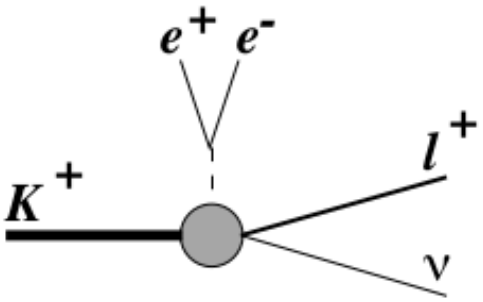

Figure 2: Structure-dependent (SD) components of the decay amplitude. [2]

where Br is the branching ratio, N stands for the actual measured counts, ε is the selection efficiency, consisting of the acceptance Acc (efficiency of the offline selection, which can be simulated by Monte Carlo (MC)), and $Trig$ which is the efficiency of the online trigger selection.

In case of a perfect MC, introducing a cut on one of the samples, its effect is precisely reproduced by simulation. This means that the difference between the measured number of events of the data with or without the cut will be relatively the same between those of the MC sample. This way these differences balance each other causing the would-be (extra) uncertainty to fall out.

A similar effect can take place if someone uses the same cuts in the signal and normalization selection, even if the effects of the cuts are not simulated perfectly in the MC. Since the cuts have the same influence on both of the data, they can mispredict the numbers of events in the same way thus in total their ratio will be the same as in case of a perfect simulation. Briefly one can say that the difference in acceptance of the signal versus the normalization cancels out, one does not have to count with new sources of uncertainty.

One has thus two ways of make the overall uncertainty small. By choosing a likely process one should count with small external uncertainty, since the likely process could be measured more precisely due to having bigger statistics. This external uncertainty has to be propagated, however, with respect to all the other sources of uncertainty (systematic or statistical) it turns out to be negligible. That is why we have chosen the channel of decaying into three pions (K3pi), it has the largest probability within three-track decays (branching ratio of 10^{-2}, while the signal Ke2ee has that of 10^{-8}).

The other possibility is to choose a decay channel very similar to the signal process. In this case one does not have to deal with significant systematic errors, because many uncertainty factors fall out if one can use the same (or similar) cuts in the signal and the normalization channel. For this case a good example is the $K^+ \to e^+ \nu \pi^0$, where $\pi^0 \to e^+ e^- \gamma$ in the so-called *Dalitz mode*), which has been studied by another member of the experiment [3]. This process has a branching ratio of about $10^{-2} \times 10^{-2}$.

1.3 The NA62 Experiment

In Figure 3 the structure of the detector system of the NA62 experiment [4] is shown.

The experiment gets protons of 400 GeV from the SPS ring smashing them to a Beryllium target (T10), from where a great diversity of particles emerge (kaon ≈6%, pion ≈70% and proton ≈24% at 750 MHz nominal beam particle rate) resulting a secondary beam of 75 GeV.

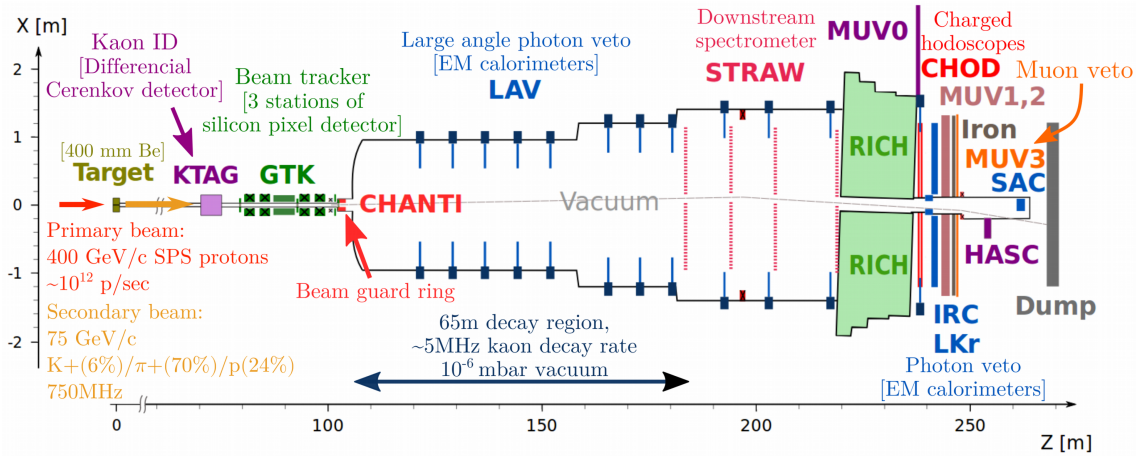

Figure 3: Structure of the NA62 experiment. [5]

One has to identify the kaons first (mainly distinguish from protons and pions in this case). This is done by exploiting the phenomena that different particles can or cannot cause Cherenkov effect in the same environment (assuming their momenta being the same within fluctuations) due to having different masses. Using this feature one can build a differential Cherenkov detector which can distinguish between the different kind of particles. The Cherenkov effect happens in a 1.6 m long tube flashed with Nitrogen (called **CEDAR**). At the end of CEDAR there are mirrors (and chromatic correctors) reflecting the Cherenkov light to the front-end readout, which is ensured by a wall of photomultipliers (PMTs) called Kaon TAGger (**KTAG**). Together, CEDAR and KTAG function as a threshold Cherenkov detector.

The experiment also has a so-called *safe volume* for emergency cases in which a leakage appears on the beam pipe. In this case Nitrogen would have been pumped to the CEDAR avoiding mechanical waves and explosion.

The next step is to track the beam, which is done by the GigaTracker (**GTK**), a Silicon pixel detector(system). It has four stations, placed between dipoles, this way deflecting particles (different kind of particles in different amount) separating types of particles as well.

Following the beamline, the next station is a rainbow-painted collimator providing veto against the *upstream events*, in which a decay is happening before the Fiducial Volume (FV, where one desires to have the kaon decay). For the same purpose was built the Charged ANTIcounter (**CHANTI**), which is a hodoscope (with plastic scintillators).

There are also several vetoes for unfavorable photons (from neutral pion decays mostly). Large Angle Vetoes (**LAV** detectors) are made of leadglass scintillators arranged in rings and are put all along the FV in certain distances from each other allowing only a forward angle region to be uncovered by them. Other electromagnetic calorimeters are placed into this region to finally cover the full viewing angle. Inner Ring Calorimeter (**IRC**) is a lead-scintillator Shashlyk detector, similarly to the Small Angle Calorimeter (**SAC**), which counts as the last LAV.

Concentrating on the decay daughters from an event of interest one can do spectrometry on the charged particles determining their momenta. The **STRAW** detector consist of four stations separated by in total of 35 m, four layers (vertical, horizontal, $\pm 45°$) of strawtube plates each. Between the two inner one, a huge magnet of 0.9 Tm is placed, giving a horizontal momentum kick of 270 MeV (which means for the beam to be deflected by 3.6 mrad).

Measuring the Cherenkov radius of charged particles one can obtain their velocity (β) by exploiting the phenomena that different types of particles have different Cherenkov radius in the same environment. Knowing also the momenta of these particles (from the STRAW), particle identification (PID) can be done trivially. The Ring Imaging CHerenkov (**RICH**) detector tube of NA62 contains Neon gas for having the Cherenkov effect, also uses mirror mosaic at the downstream end reflecting the Cherenkov light to the PM disk at the other end (horizontally at both sides of the point where the beam enters the detector).

After identifying the particles, one needs to measure their energy. Different electromagnetic and hadronic calorimeters are placed after the RICH for this purpose.

Charged HODoscope (**CHOD**) and its newer version **NewCHOD** are both hodoscopes, CHOD with planes of vertically and horizontally placed scintillator rods, while NewCHOD consist of tiles. CHOD has perfect timing, usually used as (minimum bias) trigger, while NewCHOD has a great spacial resolution.

A Liquid Kripton (**LKr**) electromagnetic calorimeter was mounted to NA62 from the NA48 experiment. It has accordion-shaped copper ribbons for cathodes and anodes in 9 m^3 liquid Kripton.

Besides the photon vetoes it is important to apply ones for muon as well. The sampling hadronic calorimeters **MUV1** and **MUV2** got their name from Muon Veto, because they help in distinguishing between muons and the hadronic pions which is a crucial task. It can be achieved with a combined usage of RICH, LKr and these MUVs, where MUV1 and MUV2 consist of iron and scintillator strips. After them (downstream) a thick wall of iron follows allowing only muons to pass it. Then, after this wall there is another MUV detector, **MUV3**, consisting of scintillators too, measuring muons.

There is another HAdronic Sampling Calorimeter (**HASC**), that together with a scintillator hodoscope (**MUV0**) are vetoeing further multitrack events (with a special condition requiring a certain minimal energy for pions, this way avoiding disturbance of noise).

2 Results

Besides exploiting the first option (choosing a very likely process for the normalization channel) to reduce uncertainty it is beneficial to use as many common cuts as possible, to reduce systematic error as well. These could be every cut obtained in the previous analysis [3] that does not belong to particle identification or the kinematic setup of the kaon decay. It is also possible in the studied case to apply both photon- and muon veto as common (general) selection criteria.

One has to also search for possible background channels that can require new cuts to avoid them. In my case the largest background component ($Br \approx 0.002$) comes from a process in which the kaon decays to a positively charged pion and a neutral pion, and this latter one decays in Dalitz mode (to an electron-positron pair and a photon). The original signal selection was already optimized against this channel, thus in this study only the stability of these cuts are examined. In the normalization channel, as it turned out, besides the multiplicity of the normalization channel its effect is still negligible, one does not need further cuts because of this background process.

Providing the cuts and their stability studies one needs to do analysis with big statistics on MC samples and analysis on measured data as well. For the MC [6], simulation samples corresponding to the experimental sets of the used full data from 2017 and 2018 data taking were used (both case all files from each list of each run available).

2.1 General Event Selection

After investigating the distributions of variables of probable cuts, I agreed to use the following general cuts listed below.

First, there are some obvious cuts, such that one is searching for one single (good) three-track positive kaon decay per burst in the FV. One also has to specify, what does "good" mean. It has to be precise enough at the first place. For what "enough" means here one can examine the χ^2 distribution of the vertex and obtain that the usual choice of $\chi^2 < 25$ is a reasonable choice now as well. Studying the time difference between the vertex (that is obtained by the CHOD) and the trigger signal (produced by RICH) one can align these detectors getting a "good" vertex. Regarding the tracks they also have to be in time with respect to the trigger (and each other).

Another trivial requirement that the reconstructed tracks have to match into the geometric acceptance of the concerned detectors.

1. only three-track events considered
2. $\chi^2_{vertex} < 25$
3. one single vertex of $|t_{vertex} - t_{trigger}| < 6$ ns
4. vertex charge $\equiv 1$
5. decay in the FV:
   105 m < reconstructed vertex position along the z (beam) axis < 180 m
6. opposit-charged particles in time with respect to the trigger:
   $|t_1^{NewCHOD} - t_2^{NewCHOD}| < 2$ ns, $|t_i^{NewCHOD} - t_{trigger}^{CHOD}| < 2$ ns
   (where i can be either 1 or 2, the label of the opposite-charged particles in any combinations)
7. geometric acceptance for the tracks (STRAW, RICH, NewCHOD, CHOD, LKr)

One has to respect the resolution of the detectors as well. LKr and STRAW have limitations concerning the ability of distinguishing two particles if they hit the detector too close to each other.

8. reasonable track separation in STRAW planes: 15 mm in each STRAW chamber
9. reasonable track separation in the LKr plane: 200 mm

Against extra activity one has to regard the time distribution of photon and muon hits with respect to the vertex time. If they are too close in time with the chosen event, one has to discard the event, since most probably it also contains an unfavoured photon as final state.

10. reject events with photons within 2 ns with respect to the t_{vertex}
11. reject events with muons within 2 ns with respect to the t_{vertex}

One can introduce further cuts assuring the good association between the detectors.

12. good association between KTAG and GTK: $|t_{GTK} - t_{KTAG}| < 1.4$ ns
13. good association between RICH and CHOD: $|t_{vertex} - t_{RICH}| < 2$ ns
14. vertex-building from the three downstream tracks and the GTK track, where the GTK candidate gives the minimal χ^2_{vertex}

Having a look at some kinematic distributions, one can choose also common cut on the tracks' momenta and the three-track momentum. The first is needed because the resolution of the STRAW looses from its reliability under / above these limits. The second one is reasonable since the reconstructed three-particle momentum cannot be higher than the momentum of the original kaon. Obviously, one has to take into account resolution issues.

15. 8 GeV < momentum of each track separately < 50 GeV
16. three-track momentum < 78 GeV

2.2 Signal Selection

For PID cuts (identifying two positrons and one electron) one has several options; one can use the calorimeters and the RICH radii.

Concerning the first opportunity, a *Boosted Decision Tree* (BDT) was used obtaining probabilities of being different kind of particles (electron, pion, muon, kaon or noise) with respect to the reconstructed signal for each track separately.

BDT is a neural network classifying particles by comparing the probability of the reconstructed signal being a specific kind of particle with a more and more strict chosen probability value (if the signal passes the comparison, it continues). The algorithm obtains the possibilities via learning complex patterns how to recognize a specific type of particles (in this case using the calorimetric data) on a huge training set.

Using the obtained probabilities one can also consider the most likely background option for each particle. Collecting their probabilities one can see how stable the prediction is (in general) for the obtained PID.

Regarding RICH likelihood one can choose from multiple quantities. These likelihoods are not probabilities in that sense that they are not normalized to one, but to the probability of the most probable candidate. Thus, besides "RICH likelihood for electron" one can study the likelihoods of all the other possibilities (pion, muon, kaon), this way checking the reliability of having a cut on "RICH likelihood for electron".

One may not need to use all of the tracks to obtain these likelihoods, probabilities. Concerning both quantities I only considered the positive tracks. In the BDT case it does not change much, while in the RICH case it is even necessary. It is because for the positive tracks it can catch most of the Cherenkov photons, while for the negative ones it looses many of them. This setup is because the main purpose of the experiment is studying $K^+ \to \pi^+ \nu \nu$ events in which only a positive particle is created (and no negative one), thus the geometry of the detector was optimized in favour to catch the positive particles. However, I used in both case only the positive tracks.

I also studied E/p (Eop) quantity from LKr, for which variable there was also a slight cut in the original selection [3]. However, it turned out that with all the other (general and signal) selections it becomes useless, the cut does not affect the numbers of selected events (not even in the data case).

17. electron probability from calorimetric BDT > 0.5 for the positive tracks

18. electron RICH likelihood > 0.5 for the positive tracks

After applying PID cuts, concerning the probable kinematic ones one can take the momentum of the neutrinos as such a quantity and applying a lower boundary on it, since one assumes to have neutrinos carrying momenta. This can be obtained by taking the difference of the reconstructed momentum of the kaon and the three-track, then calculating its magnitude.

Since GTK looses of its reliability under 8 MeV, I also cut that part.

One is interested in events in which an electron-positron pair comes from a photon. One possible background process is when the kaon decays besides the positron-neutrino pair to a neutral pion, then the pion decays in Dalitz mode. In this case the invariant mass of the electron-positron pair (from the Dalitz decay) will be related to the original pion (especially to its mass as an upper boundary). Thus applying a cut as lower boundary on this variable at / above the mass of the neutral pion, one can drop out this background option. Also, from the theoretical side, one has to use a lower energy cut avoiding divergences (due to the fact that the decay ratio grows very rapidly as one decreases the invariant mass of the electron-positron pair). Since one has to apply such a cut, it is beneficial to choose its value such that one can even neglect background events as well.

In Figure 4 on can see how powerful this cut can be regarding the right-hand side plot, where the distribution differs from the MC prediction (left-hand side plot) with a huge bulk of events at low invariant mass due to background effects that can be dropped out using the aforementioned cut.

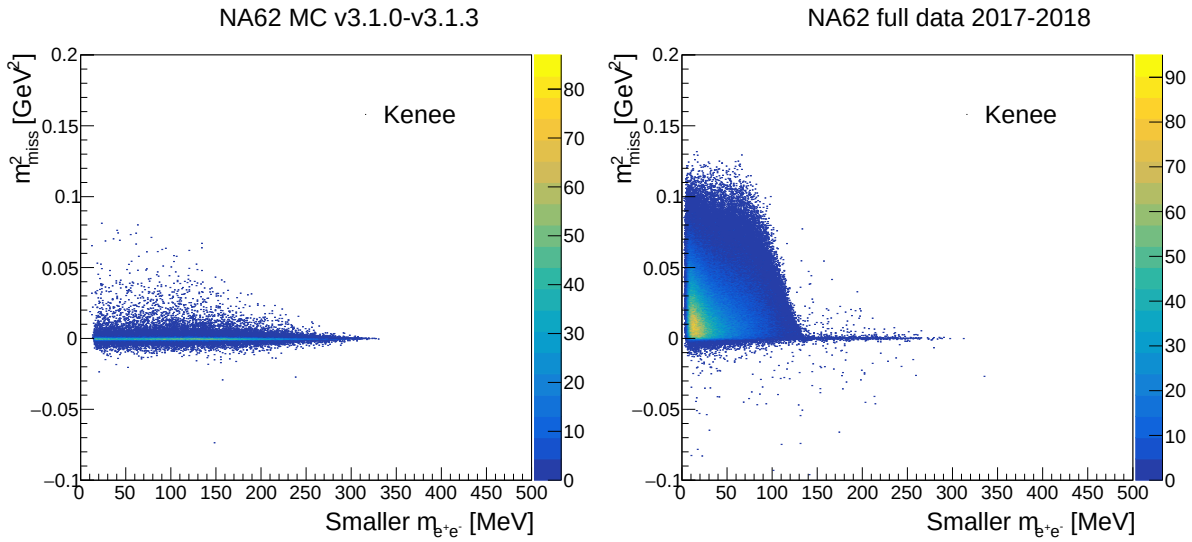

Figure 4: Squared missing mass distribution with respect to the smaller positron-electron invariant mass. Left: signal Monte Carlo sample, right: selected data.

It is worth to mention that since it is not possible to differentiate between the two (final state) positrons, it is more reasonable to search for the smaller invariant mass. This way, using a lower cut on this quantity one can be sure that it was applied on both.

Refining the selection one can have one more idea. Since the neutrinos are massless (according to the standard model), concerning missing mass one expects a well-peaked distribution around zero (as it can be seen on left-hand side of Figure 4). This way applying an upper boundary cut on this quantity (taking into account that the resolution also smears this zero to a distribution with finite width) one can further improve the selection.

20. lower boundary for neutrino momentum: $p_\nu > 200$ MeV
21. lower boundary for p_T in GTK: $p_T^{GTK} > 8$ MeV
22. lower boundary for electron-positron invariant mass: $m_{e^-,e^+} > 140$ MeV
23. upper boundary for missing mass: $m^2_{miss} < 0.03$ GeV^2

2.3 Normalization Selection

Several possibilities for normalization selection has been also studied.

Regarding the PID the same possibilities were examined as were in the signal case (obviously changing the particle of interest from electron to pion). Moreover, I considered the total RICH probability not to being pion and the maximum RICH probability of not being pion (including noise probability).

Finally I decided to not use any PID criteria in the normalization selection, since due to the high branching ratio, the normalization data sample is already a good enough sample for K3pi events and introducing new cuts would also mean new sources of uncertainty.

Concerning kinematics the most reasonable variable for a cut is the reconstructed three-pion mass, which is well-peaked around the official value [7] of the kaon mass, 493.677 ± 0.013 MeV (Figure 5).

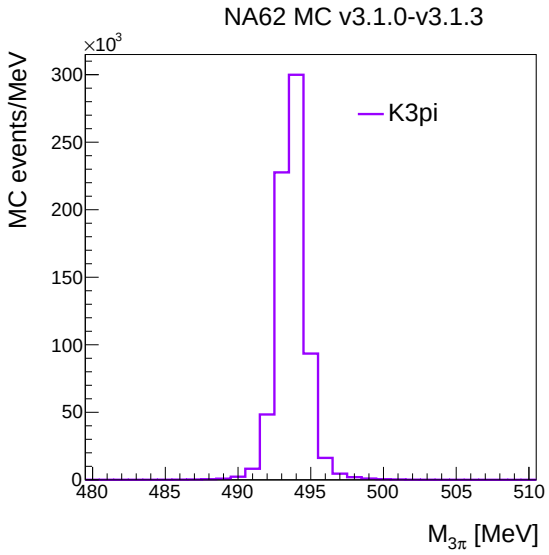

Figure 5: Three-pions invariant mass reconstructed from the K3pi MC.

Using this feature one can have a strict enough condition obtaining most of the normalization events and getting rid of most of the non-normalization ones.

24. kaon invariant mass reconstructed from the three tracks compatible with the kaon mass: $|m_{3\pi} - m_{K^+}| < 4$ MeV

Regarding the data sample, there different *trigger masks* [8] were used due to the different frequency of the considered processes, but the cuts applied in the MC obviously have to be used there too.

For the various specific processes multiple additional constraints are used at trigger level, these are the trigger masks. For the normalization channel at the very first, low-level trigger (L0) the *multi-track* mask was used based on RICH signal multiplicity and requiring two opposite NewCHOD quadrants to fire (in coincidence). It also means a *downscaling* of 100.

For the signal one needs another mask, the *di-electron* one, requiring besides the multi-track conditions a minimum of 20 GeV energy deposit in the LKr. It is a stronger condition with respect to the multi-track one, meaning less events remained that can be caught in the downscaling, which is in this case around 8.

Concerning the MC sample it is also useful to separate signal / normalization sets in the sense that if an event was analyzed in the signal selection part, it is important not to allow it to be analyzed in the normalization selection again. Thus, I used an extra cut in the normalization selection, the inverse condition of the original EoP requirement (in the signal selection), since that proved to be always true there, this way I assured a perfect separation. Also it is a very loose condition for pions, thus I did not lose on statistics.

19. EoP from LKr < 0.9

2.4 Stability studies

One can never know in advance if the used MC was sensitive to a quantity or not. If the quantity is not well simulated, using a cut on it behaves differently on MC sample than on measured data. Thus it is important to check how the branching ratio behaves if one changes the cut value.

It is important to examine this for only (but all of) those cuts that are different between the selection and the normalization (not present in one of them), since for those that are the same (used in both cases) this effect falls out.

It is also beneficial to normalize the branching ratios to that value that was obtained with the chosen cut value (*central value*). This way, for the other cut values one can represent uncertainty only considering the number of different events with respect to the central value (using Poissonian fluctuation), this is the so-called *uncorrelated error*. For the central value I shown the real error within which all the other values have to fit within their uncertainty (representing the uncertainty on the variation) as it can be seen on the Figures 6- 7 shown below.

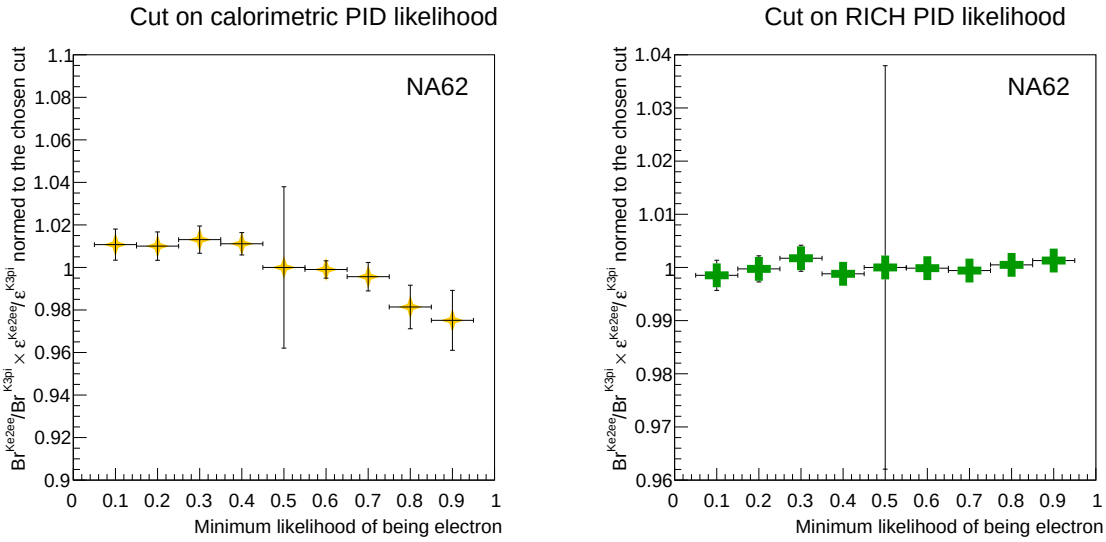

Figure 6: Stability studies on PID cuts.

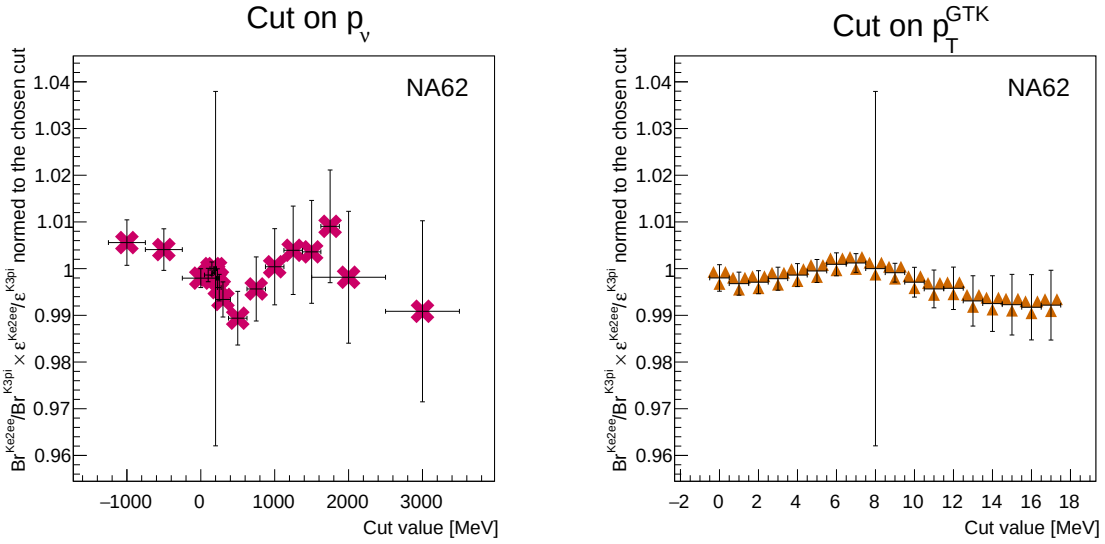

Figure 7: Stability studies on kinematic cuts.

Regarding Figure 8 one can see how powerful is the cut on the (smaller) electron-positron invariant mass. Taking only a loose requirement there are much more "signal" events left (mainly misidentified background), that is why the values tend to diverge on the plot in the top left corner.

On the other hand, regarding the too strict cuts, one can hardly find events (on the plot in the top right corner the last datapoint refers to only eight signal events in the data, on the plot in the bottom left corner the last ones from right to left had 194, 385, 543 with respect to 708 in the case of the chosen cut value). This way one gets enormous uncertainties and unreliable values, thus these datapoints I neglected on the plot in the bottom right corner validating that changing the cut value one can get a result still comparable to that of obtained by the chosen cuts within uncertainty, the cut is indeed stable enough.

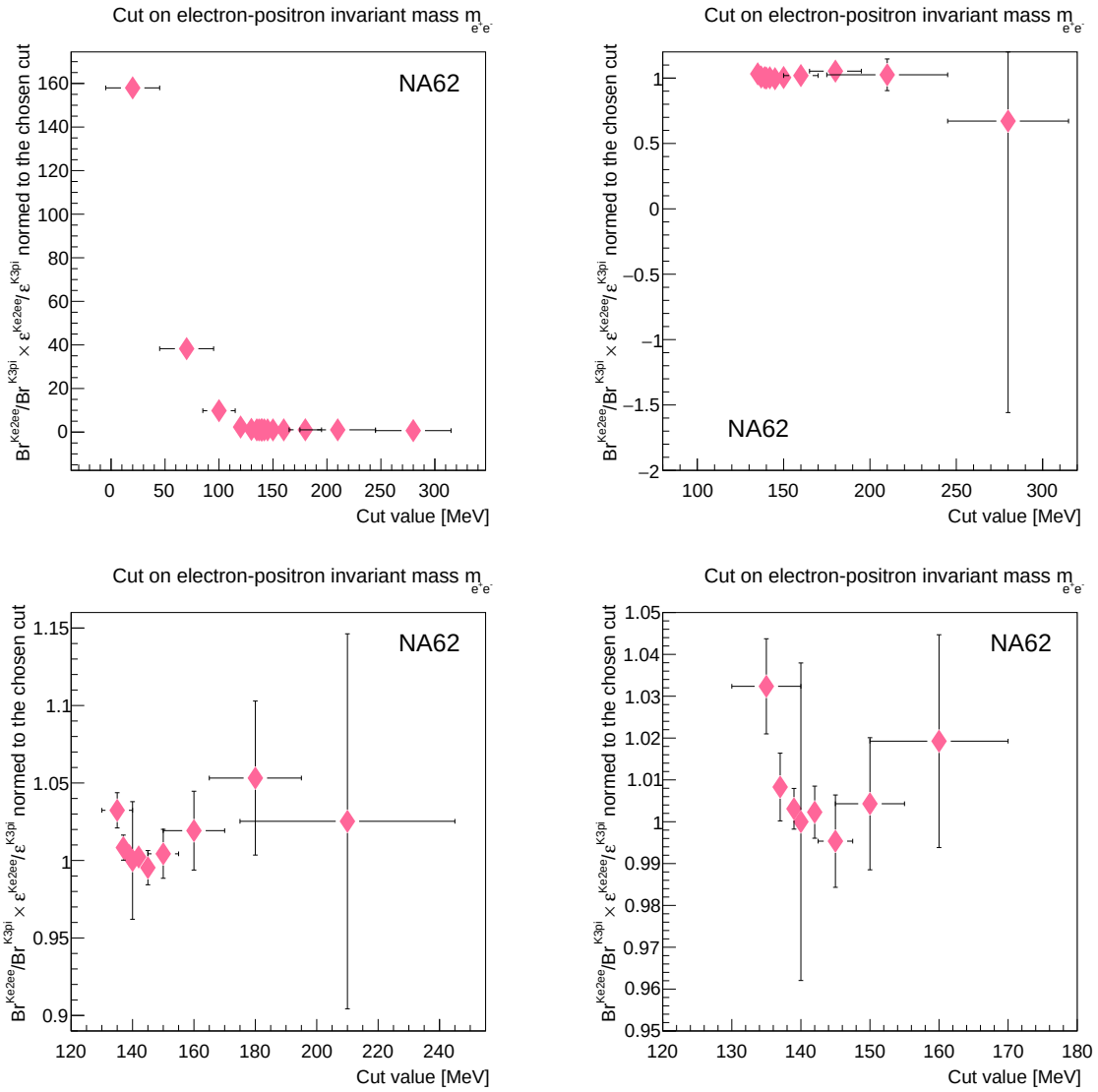

Figure 8: Stability studies on the cut of the smaller invariant mass of the electron-positron pairs. All plots show the same data zoomed differently.

While for the normalization case the cut for the kaon invariant mass is perfectly stable, another kinetic cut, in the signal case seems to be much less stable (Figure 9). This is the cut for the missing mass. Generally speaking if the branching fraction depends much on the cut value, it is safer to choose the cut (if its presence is necessary) to a flatter region. Luckily, one can find such a region here as well, just at the vicinity of the originally chosen cut value.

Also, carefully looking at the plot one can spot that those outliers are about one order of magnitude below the chosen value that would mean a too strong requirement for this quantity on the basis of Figure 4 as well.

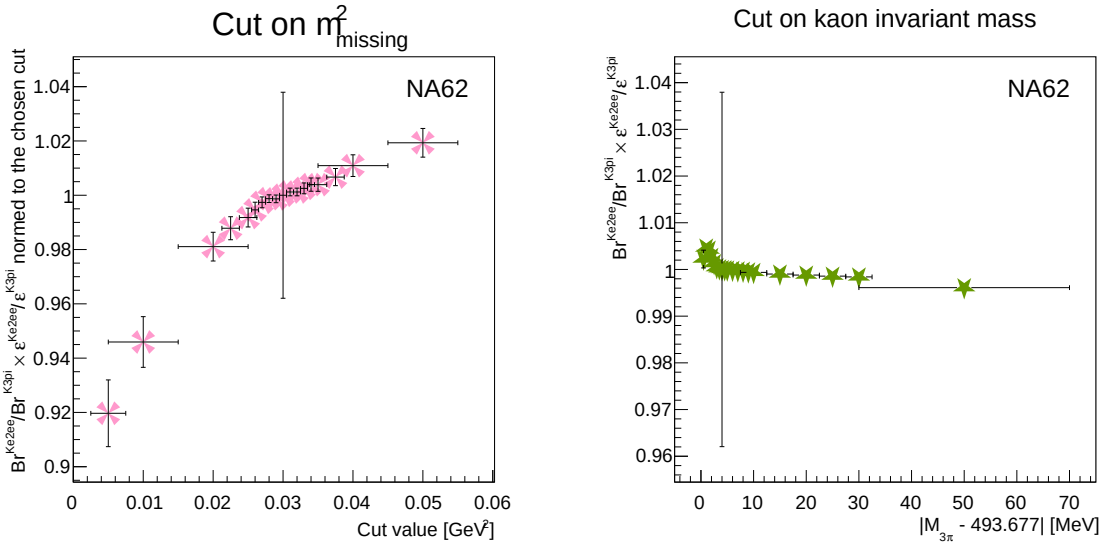

Figure 9: Stability studies on different kinematic cuts. Left: on the signal set, right: on the normalization set.

2.5 Trigger efficiency

Trigger efficiency is defined with respect to the actual selection. This means that one has to study the number of remained events on the basis of the concerned triggers after the event selection. In case of a perfect trigger one would have the same number of event with or without the extra requirement of a firing trigger as without that. In reality it can happen that even if the offline selection reproduced the trigger selections, after all selection cut one will get less event with requiring also signal from the actual trigger than without it. In this case the trigger is not efficient.

It is very important to know how inefficient the used triggers are. One can obtain this from data using an independent trigger, or estimate it from MC. In my case since the signal selection use strict criteria, regarding the control trigger, due to its strong downscaling I have got only 11 events from the full dataset matching to both the signal (+general) selection criteria and that of having the control trigger firing. With respect to the 708 events from the signal selection it would make no sense using these data due to low statistics.

Thus finally I estimated trigger efficiency from MC, where one has to emulate the signal of the hardware-level online (L0) triggers. From this I could conclude that (see in more details in Table 1) the extra condition in the signal case (LKr20 that requires a minimum of 20 MeV energy deposited in the LKr) has a very small inefficiency.

3 Conclusion

During my work my goal was to build an event selection for the $K^+ \to e^+ \nu e^+ e^-$ signal decay with using $K^+ \to \pi^+ \pi^+ \pi^-$ as normalization channel and check the stability of the applied cuts.

I obtained an event selection (competing with a similar one using $K^+ \to e^+ \nu \pi^0$, $\pi^0 \to e^+ e^- \gamma$ as normalization channel) exploiting the amount of statistics in the normalization case due to being the most likely process among the three-track events.

I also studied the stability of the cuts, where they all proved to be stable enough in the region where they are used.

Speaking in numbers one can see the results in Table 1. Knowing that the branching ratio of the normalization channel is $(5.583 \pm 0.024)\%$ [7], the obtained branching ratio for the signal is $(\mathbf{3.13 \pm 0.12}) \cdot \mathbf{10^{-8}}$, which, with respect to the recent value in the literature ($3.39 \cdot 10^{-8}$ [1], both for the $m_b e^-, e^+ > 140$ MeV case) can be concerned as a good enough result.

Table 1: Branching ratio for the rare decay $K^+ \to e^+ \nu e^+ e^-$ (Ke2ee) using $K^+ \to \pi^+ \pi^+ \pi^-$ (K3pi) as normalization channel.

	Signal	**Normalization**	**Ratio**
N	708±26.61	230419472±15180	$(3.073 \pm 0.116) \cdot 10^{-6}$
Acc	0.02837±0.00015	0.06300±0.00008	2.221±0.012
ε	0.9265±0.0069	0.9126±0.0017	0.9851±0.0076

4 Acknowledgement

I would like to thank at the first place my supervisors, Francesco Brizioli and Monica Pepe, for the fantastic opportunity of being at CERN in general and especially at the NA62 experiment, also for the interesting topic I enjoyed very much working on. I would like to highlight the help of Francesco Brizioli with his patient explanations, kindness, many advices with the coding and technical details of the detector that I had the opportunity to visit in person for which I am also much obliged to Him and to the Collaboration. I also would like to thank the Collaboration in general for paving my way and making me able to be a part of such an amazing experiment. I further would like to thank the support of the organizers and the whole program, including the lectures, workshops and visits, where too, I had the honour to learn a lot from the experts. I am grateful for this incredible Summer also to fellow Summer Students making our leisure time fun and unforgettable.

References

[1] J. Bijnens, G. Ecker, J. Gasser, Radiative Semileptonic Kaon Decays, *Nucl. Phys. B*, **1992**, *396*, 81-118.
DOI: 10.48550/arXiv.hep-ph/9209261

[2] A. A. Poblaguev, R. Appel, G. S. Atoyan, B. Bassalleck, D. R. Bergman, N. Cheung, S. Dhawan, H. Do, J. Egger, S. Eilerts, W. Herold, V. V. Issakov, H. Kaspar, D. E. Kraus, D. M. Lazarus, P. Lichard, J. Lowe, J. Lozano, H. Ma, W. Majid, S. Pislak, P. Rehak, A. Sher, J. A. Thompson, P. Truöl, and M. E. Zeller, Experimental Study of the Radiative Decays $K^+ \to \mu^+ \nu e^+ e^-$ and $K^+ \to e^+ \nu e^+ e^-$, *Physical Review Letters*, **2002**, *89*, 6.
DOI: 10.1103/PhysRevLett.89.061803

[3] G. Romolini, Study of the $K^+ \to e^+ \nu e^+ e^-$ decay with the NA62 experiment at CERN.
Restricted availability here.

[4] E. Cortina Gil et al., The beam and detector of the NA62 experiment at CERN, *JINST*, **2017**, *12*, P05025. DOI: 10.1088/1748-0221/12/05/P05025

[5] M. B. Brunetti, F. Gonnella, L. Iacobuzio, on behalf of the NA62 Collaboration, Search for Exotic Particles at the NA62 Experiment, *Universe*, **2018** *4(11)* 119.
DOI: 10.3390/universe4110119

[6] NA62-specific Monte Carlo data sample for the signal (*kenuee*), normalization (*k3pi*) and the most prominent background (*k2pi.pi0d*).
Restricted availability here.

[7] M. Tanabashi et al. (Particle Data Group), Charged Kaon Mass, *Phys. Rev. D*, **2018**, *98*, 030001.
DOI: 10.1103/PhysRevD.98.030001

[8] The NA62 Collaboration, Searches for lepton number violating K^+ decays, *Physics Letters B*, **2019**, *797*, 134794.
DOI: 10.1016/j.physletb.2019.07.041